

REVISITING CANNABINOID RECEPTOR 2 EXPRESSION AND FUNCTION IN MURINE RETINA

Joanna Borowska-Fielding², Natalia Murataeva¹, Ben Smith³, Anna-Maria Szczesniak², Emma Leishmann¹, Laura Daily¹, Tom Toguri², Cecelia Hillard⁴, Julian Romero⁵, Heather Bradshaw¹, Melanie Kelly^{2,3,6}, Alex Straiker¹

Department of Psychological and Brain Sciences, Gill Center for Biomolecular Science¹, Indiana University, Bloomington, IN, USA

Departments of Pharmacology², Physiology and Biophysics³, Anesthesia⁶, Ophthalmology and Vision Sciences⁴, Dalhousie University, Halifax, NS, Canada. ⁴Department of Pharmacology and Toxicology, Medical College of Wisconsin, Milwaukee, WI, USA.

⁵Neuroimmunology Group, Neural Plasticity Department, Cajal Institute, Consejo Superior de Investigaciones Científicas, 28002 Madrid, Spain

Corresponding author:

Alex Straiker

1101 E 10th Ave

Bloomington, IN 47401

Tel: (206) 850 2400

Email: straiker@indiana.edu

ABSTRACT

The cannabinoid receptor CB2 plays a significant role in the regulation of immune function whereas neuronal expression remains a subject of contention. Multiple studies have described CB2 in retina and a recent study showed that CB2 deletion altered retinal visual processing. We revisited CB2 expression using immunohistochemistry and a recently developed CB2-eGFP reporter mouse. We examined the consequence of acute vs. prolonged CB2 deactivation on the electroretinogram (ERG) responses. We also examined lipidomics in CB2 knockout mice and potential changes in microglia using Scholl analysis. Consistent with a published report, in CB2 receptor knockout mice see an increased ERG scotopic a-wave, as well as stronger responses in dark adapted cone-driven ON bipolar cells and, to a lesser extent cone-driven ON bipolar cells early in light adaptation. Significantly, however, acute block with CB2 antagonist, AM630, did *not* mimic the results observed in the CB2 knockout mice whereas chronic (7 days) block did. Immunohistochemical studies show no CB2 in retina under non-pathological conditions, even with published antibodies. Retinal CB2–eGFP reporter signal is minimal under baseline conditions but upregulated by intraocular injection of either LPS or carrageenan. CB2 knockout mice see modest declines in a broad spectrum of cannabinoid-related lipids. The numbers and morphology of microglia were unaltered. In summary minimal CB2 expression is seen in healthy retina. CB2 appears to be upregulated under pathological conditions. Previously reported functional consequences of CB2 deletion are an adaptive response to prolonged blockade of these receptors. CB2 therefore impacts retinal signaling but perhaps in an indirect, potentially extra-ocular fashion.

Key Words:

Cannabinoid, CB2, retina, electroretinogram, ERG

Abbreviations:

ERG, electroretinogram; GFP, green fluorescent protein; GCL, ganglion cell layer; IPL, inner plexiform layer; INL, inner nuclear layer; KO, knockout; LPS, lipopolysaccharide; OPL, outer plexiform layer; PG, prostaglandin.

INTRODUCTION

Of the two canonical cannabinoid receptors (CB1 and CB2), CB1 receptors are expressed in the synaptic layers of the retina in species ranging from salamander to primate (Straiker et al., 1999a; Straiker et al., 1999b) where they have been shown to alter neuronal function in both photoreceptors and bipolar cells (Straiker et al., 1999a; Straiker and Sullivan, 2003). The question of whether CB2 receptors are also expressed in retina has swung pendulum-like from initial studies that mostly failed to detect CB2 ((Buckley et al., 1998; Porcella et al., 1998; Porcella et al., 2000) vs. (Lu et al., 2000)) to a consensus for functional CB2 in retina based on a growing number of publications. This includes immunohistochemical evidence (Bouskila et al., 2013; Cecyre et al., 2014; Cecyre et al., 2013; Lopez et al., 2011; Maccarone et al., 2016), and studies showing altered electroretinogram responses involving CB2 receptor function in mouse (Cecyre et al., 2013; Imamura et al., 2018). There is evidence that CB2, long associated with immune function (Atwood et al., 2012), regulates ocular inflammation (reviewed in (Toguri et al., 2016)) and there is evidence for retinal neuroprotection as a consequence of CB2 activation (Imamura et al., 2018) or antagonism (Maccarone et al., 2016). With this growing body of evidence the presence of functional CB2 receptors in the retina seems certain, particularly since two studies used knockout controls (Cecyre et al., 2014; Cecyre et al., 2013). However a definitive localization for CB2 remains elusive since the expression studies of Lopez et al. and Cecyre et al., Bouskila et al., Maccarone et al., and Lu et al. each shows different localization for CB2. The difference between these studies may be due to species-related differences (rat, mouse and vervet monkey) but this is surprising given the general conservation of retinal structure across species. Even the studies carried out in mice, Cecyre et al., Maccarone et al., and Lu et al. are inconsistent with one another. It should be noted that the cannabinoid field has struggled with a consistent lack of specificity among the numerous CB2 antibodies that have

been developed and tested (reviewed in (Atwood and Mackie, 2010; Atwood et al., 2012)). Still, the subsequent finding using electroretinograms (ERGs) that CB2 (but not CB1) deletion alters retinal signaling (Cecyre et al., 2013) reinforced the idea that there is a CB2-based cannabinoid signaling system that directly modulates the retinal output. These findings had implications for the general question of functional CB2 in neurons - itself a subject of debate – since the evidence for functional CB2 in neurons has rested largely on the work of two groups, one working in the hippocampus and ventral tegmental area (Zhang et al., 2016) and one working in the retina (Bouskila et al., 2016; Cecyre et al., 2014; Cecyre et al., 2013).

We have revisited the question of CB2 presence and function in the retina in somewhat greater detail, using a combination of ERGs, lipidomics, immunohistochemistry and a novel CB2-eGFP reporter mouse.

METHODS

Animals

C57BL/6J (WT) and CB2R KO mice (C57BL/6J, background strain) were used for all experiments except the lipidomics analyses that used CB2 KO mice back-crossed onto a BALB/c background, compared to BALB/c strain-mates. Experimental procedures performed in Canada complied with Canadian Council on Animal Care (<http://www.ccac.ca>). Experiments were approved by respective animal care committees at Dalhousie University and Indiana University.

Immunohistochemistry

For CB2 antibody testing the following procedure was followed. Adult mice (C57/BL6 strain, > 5 weeks, of either sex, from breeding colony) were housed under a 12/12 hour day/night cycle, then sacrificed. Eyes were removed, and the anterior eye section cut away and the lens extracted, leaving an eyecup. For immunocytochemistry, the posterior eyecup was fixed in 4% paraformaldehyde for an hour followed by a 30% sucrose immersion for 24-72 hours at 4°C. Tissue was then frozen in OCT compound and sectioned (15-25 µm) using a

Leica CM1850 cryostat. Tissue sections were mounted onto Fisher Superfrost-plus slides, washed, blocked with SEABLOCK blocking buffer (Thermo Fisher) for 30 minutes, treated with a detergent (Triton X-100, 0.3% or saponin, 0.1%), followed by primary antibodies overnight at 4 °C. Anti-CB2 polyclonal antibodies were obtained as listed in Table 1. To visualize microglia, retinas were stained with primary antibodies Anti-Iba-1 Polyclonal Antibody (Cat: 019-19741; 1:200, Wako Chemicals USA). eGFP signal was detected using a pre-labeled anti-GFP antibody (Alexa647-labeled, Cat#: A-31852 ThermoFisher). Secondary antibodies (Alexa488, Alexa 594 or Alexa647, 1:500, Invitrogen) were subsequently applied at room temperature for 1.5 hours. Microscopy was carried out at Indiana University and images were acquired with a Leica TCS SP5 confocal microscope (Leica Microsystems, Wetzlar, Germany) using Leica LAS AF software and a 40x or 63x oil objective. Images were processed using FIJI (<https://imagej.net/Fiji/>, provided in the public domain by the National Institutes of Health, Bethesda, MD, USA) and Photoshop (Adobe, Inc., San Jose, CA, USA). Images were modified only in terms of brightness and contrast.

Table 1. Commercial CB2 antibodies tested

Antibody	Host	Vendor	Cat #	Lot number
CB2	Rabbit	Abcam	ab3561	GR145565-3, GR209773-1
CB2	Rabbit	Cayman Chemical Company	101550	0437 135-1
CB2	Rabbit	Affinity Bio Reagents	PA1-744	423-107
CB2R	Rabbit	Alomone Labs	ACR-002	AN-01
CB2 (M-15)	Goat	Santa Cruz Biotechnology	SC-10076	E2314

Scholl analysis of Iba1-stained microglia was done using the FIJI plugin Simple Neurite Tracer (Longair et al., 2011) to map out the morphology of the microglial cell in three dimensional space and calculate the number of process crossings at 5 micron intervals.

Generation of CB₂R-GFP Reporter Mice

Generation of CB₂R-GFP reporter mice has been described (Lopez et al., 2018). Briefly an eGFP reporter gene preceded by an IRES sequence in the 3' UTR of the *CNR2*, (CB2) mouse gene was inserted into the embryonic stem cells of C57BL/6j mice resulting in the

expression of the reporter gene under the control of the endogenous mouse CB₂R promoter and transcription from the same bicistronic mRNA as the CB₂R protein. The mouse model (CB₂R eGFP/f/f) was generated by homologous recombination in embryonic stem cells, in the C57BL/6J genetic background.

Intraocular injections

Mice were first injected with an analgesic (0.05 mg/kg buprenorphine, IP), followed by general isoflurane anesthesia. While the animal was anesthetized, intravitreal injection of either saline, or LPS in saline, was given through the pars plana, under a dissecting stereomicroscope using a Hamilton syringe fitted to a 30G needle. Control animals received 2 µL of sterile saline, while experimental animals are injected with 250 ng lipopolysaccharide (LPS; 125 ng µL⁻¹; E. coli 026:B6 L8274; Sigma-Aldrich) in 2 µL of saline. The animal was allowed to revive then monitored for three hours, after which the animal was euthanized and the eyes collected for analysis of GFP expression. The procedure for carrageenan was the same except that a 1.5% solution of carrageenan was used.

Electroretinography

The function of CB₂ receptors in the retina was investigated by recording electroretinographic responses (ERGs) under light conditions designed to isolate rod and cone driven responses under dark (scotopic), and light adapted (photopic) conditions. We tested CB₂R KO vs. wild type animals, and additionally tested the consequence of administration of CB₂ receptor antagonist AM630 (2.5mg/kg, IP). AM630 experiments consisted either of a single treatment or a chronic treatment (7 days, twice a day, every 12h intraperitoneal injection).

Electroretinographic protocols have been described in detail elsewhere (Smith et al., 2013). Briefly mice between 13 and 17 weeks of age were dark-adapted for 8-12h overnight and anesthetized under dim red light by intraperitoneal injection of Avertin (2,2,2 Tribromoethanol) dissolved in amylene hydrate (tertiary amyl alcohol, 275 mg/kg). Pupils were dilated with 1% tropicamide (mydriacyl); a topical analgesic was applied to reduce eye movement and irritation. Body temperature was maintained at 37°C with a heated pad and monitored rectally. Mice were sacrificed by anesthetic overdose followed by cervical

dislocation. The interval between stimuli varied between 15 s for paired flash experiments to 1 s for light-adapted stimuli. 5–20 responses were averaged depending on stimulus strength. Paired flash stimuli to isolate dark-adapted cone responses used a 500 ms inter-flash interval. ERG waveform analysis was performed according to the standard method (McCulloch et al., 2015). The a-wave amplitude was measured from baseline to the trough of the a-wave and the b-wave amplitude was measured from the trough of the a-wave to the positive peak of the b-wave. Statistical analysis was performed by using unpaired t-test and two-way ANOVA followed by Bonferroni post hoc test. Experimental values were presented as means \pm SEM; * $P \leq 0.05$; ** $P \leq 0.01$; *** $P \leq 0.001$; **** $P \leq 0.0001$.

Lipid Extraction and LC/MS/MS Analysis and Quantification

Enucleated eyes were flash frozen in liquid nitrogen and frozen at -80°C until used for lipid analysis. Levels of ~30 cannabinoid-related lipids as well as arachidonic acid and several prostaglandin-family metabolites were measured by liquid chromatography/mass spectrometry from whole eyes as previously described (Bradshaw et al., 2009). Briefly, eyes from six animals for each condition (two eyes pooled as one sample) were homogenized, centrifuged at $19,000 \times g$ 24°C for 20 min and supernatant was collected. Compounds were isolated using a partial purification of the 25% organic solution. C18 solid-phase extraction columns (Agilent Technologies, Santa Clara, CA) were used with an elution of 100% methanol.

Samples were placed in an autosampler and held at 24°C (Agilent 1100 series autosampler, Palo Alto, CA) for LC/MS/MS analysis. 10–20 μL of eluents were injected for each sample which was rapidly separated using a C18 Zorbax reversed-phase analytical column (Agilent Technologies, Santa Clara, CA) to scan for individual compounds. Gradient elution (200 $\mu\text{L}/\text{min}$) then was accomplished under pressure (Shimadzu 10AdVP pumps, Columbia, MD). The electrospray ionization was done using an API3000 triple quadrupole mass spectrometer (Applied Biosystems/DSM Sciex, Foster City, CA). A multiple reaction monitoring (MRM) setting on the LC/MS/MS was used to analyze levels of each compound. Synthetic standards were used to generate optimized MRM methods and standard curves for analysis.

Individual animals in each of the treatment groups were coded and experiments were analyzed in a blinded fashion. All data are presented as mean \pm SEM and were analyzed in GraphPad Prism v. 5 (GraphPad Software Inc., La Jolla, CA, USA). LC/MS/MS lipidomics data was analyzed by one-way ANOVA with a Fisher's Least Significant Difference *post-hoc* test. All groups were normally distributed according to the Kolmogorov-Smirnov test. $P < 0.05$ was considered statistically significant.

RESULTS

Revisiting CB2 immunohistochemistry in retina

Cecyre et al. (Cecyre et al., 2014; Cecyre et al., 2013) tested multiple antibodies against CB2 to characterize protein expression in retina. These studies used knockout controls and identified one of the antibodies as delivering staining that was absent in knockout tissue, i.e. a validated CB2 antibody. Pronounced expression was seen in both synaptic layers, in the ganglion cell layer and also in photoreceptor inner segments. All staining was absent in CB2 knockout retinas. This antibody, from Cayman Chemical (See Table 1 for details) was obtained by us and tested in murine retina, also using knockout controls.

As reported by Cecyre et al. (Cecyre et al., 2014), the staining was most prominent in the inner plexiform layer (Fig. 1, IPL). The staining we observe for this antibody is both similar to that reported by Cecyre et al., and to the staining in knockout controls and therefore inconsistent with valid CB2 expression. We also tested a variety of other commercially available CB2 antibodies (Table 1) but none offered staining that was absent in CB2 KO tissue (Figure S4). As noted in the introduction the specificity of CB2 antibodies has been a persistent issue since the receptors were first identified. This has prompted the development of alternative strategies to identify where these receptors are expressed including CB2-eGFP reporter mice.

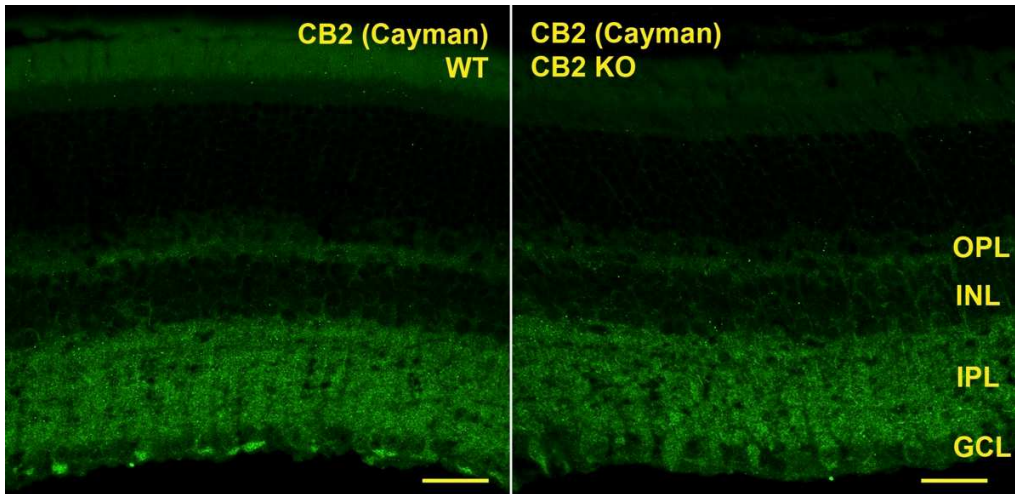


Figure 1. Cayman CB2 antibody yields similar staining in WT and CB2 knockout tissue. A) CB2 antibody staining in retina using Cayman Chemical antibody previously validated in knockout controls by Cecyre et al. (2013, 2014). B) Staining for CB2 in knockout tissue is nearly identical with the exception of staining in the GCL layer. Scale bars: 50 μ m.

Minimal signal in baseline CB2-eGFP reporter mice is upregulated after intraocular injection of LPS or carrageenan.

The CB2-eGFP mouse model was developed to offer an alternative assay for CB2 expression. Designed to produce eGFP untethered to CB2 but under a CB2 promoter (Lopez et al., 2018), this CB2-eGFP reporter mouse identifies which cells express CB2 but not where within a cell CB2 is expressed. As shown in Figure 2A only minimal eGFP staining is seen in murine retina. We occasionally observed dim microglia-like staining in the INL but the staining is sparse, representing a small subset of microglia. Because of the immune-CB2 link we tested whether an inflammatory insult might upregulate CB2 expression. We tested the consequence of intraocular injection of LPS and in a separate experiment carrageenan (Toguri et al., 2015). As shown in Figures 2B,D each treatment resulted in a substantially enhanced eGFP signal particularly in the ganglion cell layer but also to a lesser extent in the proximal inner nuclear layer. The staining appears to correspond to golgi or endoplasmic reticulum, presumably as a result of rapidly upregulated expression in response to inflammatory insult.

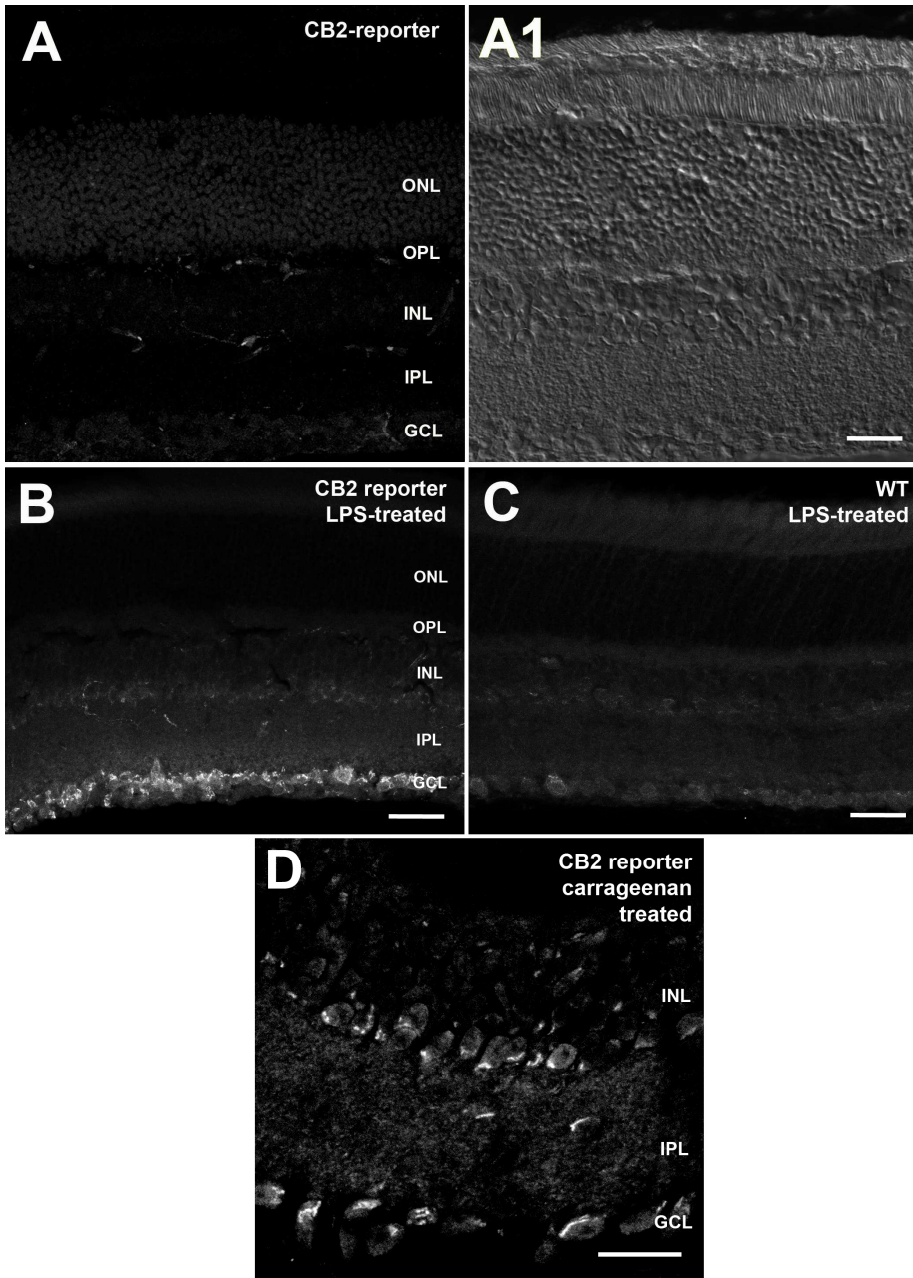


Figure 2. CB2 is upregulated from low baseline levels by LPS/carrageenan in murine retina. A) GFP staining is minimal in CB2-eGFP reporter mouse. A1) corresponding DIC image. B-C) Intraocular LPS injection induces an eGFP signal in CB2-eGFP reporter (B) but not in WT (C) mice. B&C were taken at same settings in single microscopy session to allow for comparison. D) Carrageenan injection results in similar upregulation of GFP. Scale bars: 20 μ m

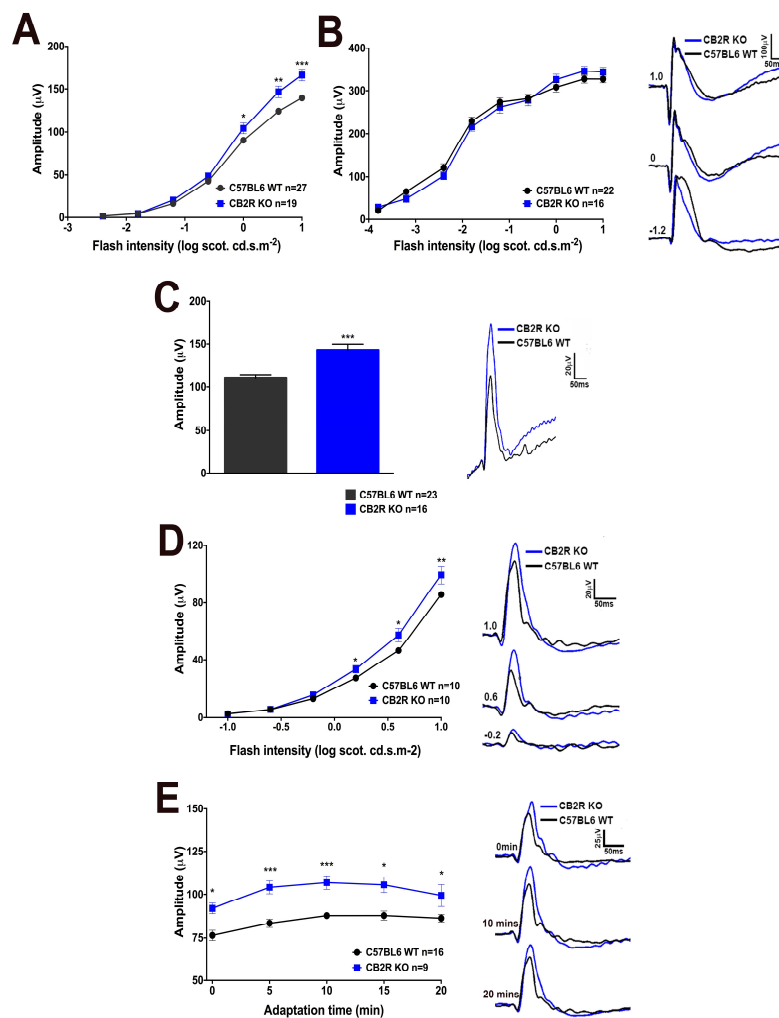


Figure 3. ERG responses are altered in CB2 KO mice relative to wild type controls A-B) Amplitudes of scotopic ERG a-wave (A) and b-wave (B) plotted as a function of flash luminance. C) Amplitudes of scotopic ERG dark-adapted cone-driven response after rod saturation. D) The amplitudes of photopic ERG b-wave are plotted as a function of flash luminance. E) The amplitudes of photopic ERG b-wave are plotted as a function of time. *, $p < 0.05$, **, $p < 0.01$, ***, $p < 0.001$, 2-way ANOVA with Bonferroni post hoc test

ERG responses are altered in CB2 KO mice relative to wild type controls

Consistent with previous findings (Cecyre et al., 2013), we see an alteration of the ERG response profile in CB2 knockout mice vs. strain controls. The scotopic a-wave is significantly increased (*, $p < 0.05$ to ***, $p < 0.001$) at higher stimulus strengths in CB2 knockouts while the b-wave is not (Fig. 3B). In dark-adapted conditions the cone-driven response is also significantly increased (Fig. 3C). The cone-driven b-wave remained significantly elevated during light adaptation and when fully light adapted, the b-wave is increased above $-0.2 \log \text{cd m s}^{-2}$ (***, $p < 0.001$).

During light adaptation we found that the b-wave responses were also modestly enhanced in CB2 knockouts

relative to wild type mice (Fig. 3D). We also examined whether this changed over time as

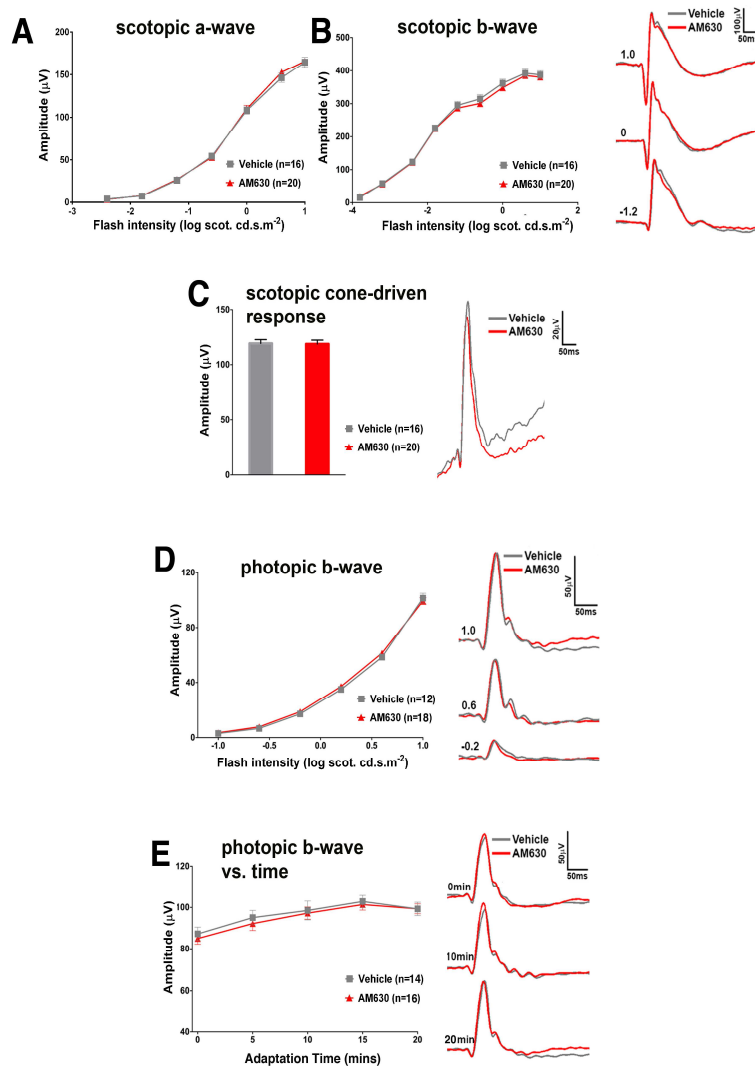


Figure 4. Acute treatment with CB2 antagonist does not mimic alteration of ERG seen in CB2 KO mice. Animals were treated with a CB2 antagonist AM630 (2.5 mg/kg, IP). A-B) Amplitudes of scotopic ERG a-wave (A) and b-wave (B) plotted as a function of flash luminance. C) Amplitudes of scotopic ERG dark adapted cone-driven response after rod saturation. D) The amplitudes of photopic ERG b-wave are plotted as a function of flash luminance. E) The amplitudes of photopic ERG b-wave are plotted as a function of time. *, $p < 0.05$, **, $p < 0.01$, ***, $p < 0.001$, 2-way ANOVA with Bonferroni post hoc test

the animals were light-adapted, finding that the difference was maintained for 15 minutes, though it was no longer statistically significant at 20 mins. We additionally examined whether CB2 deletion altered the latencies of ERG responses. We found that CB2 KO mice did not have altered latencies (Fig. S1). The sole exception was a shorter latency in CB2 KOs at the highest flash intensity Fig. S1C).

Acute pharmacological blockade of CB2 receptors does not mimic the ERG alterations seen in CB2 KO mice

If CB2 participates in an active retinal signaling system, and CB2 deletion alters retinal signaling, then one would predict that an antagonist of CB2 would similarly alter signaling. We therefore tested the

ERG responses in wild type mice treated with the CB2 antagonist, AM630 (2.5mg/kg, IP). Surprisingly, we found that this treatment was without any effect on either scotopic or photopic responses (Fig. 3) even though similar concentrations were found to block CB2 activation in rats and mice (Lehmann et al., 2012; Toguri et al., 2014). We also examined whether acute AM630 treatment altered the latencies of ERG responses, finding that there was no effect of a single treatment with AM630 (Fig. S2).

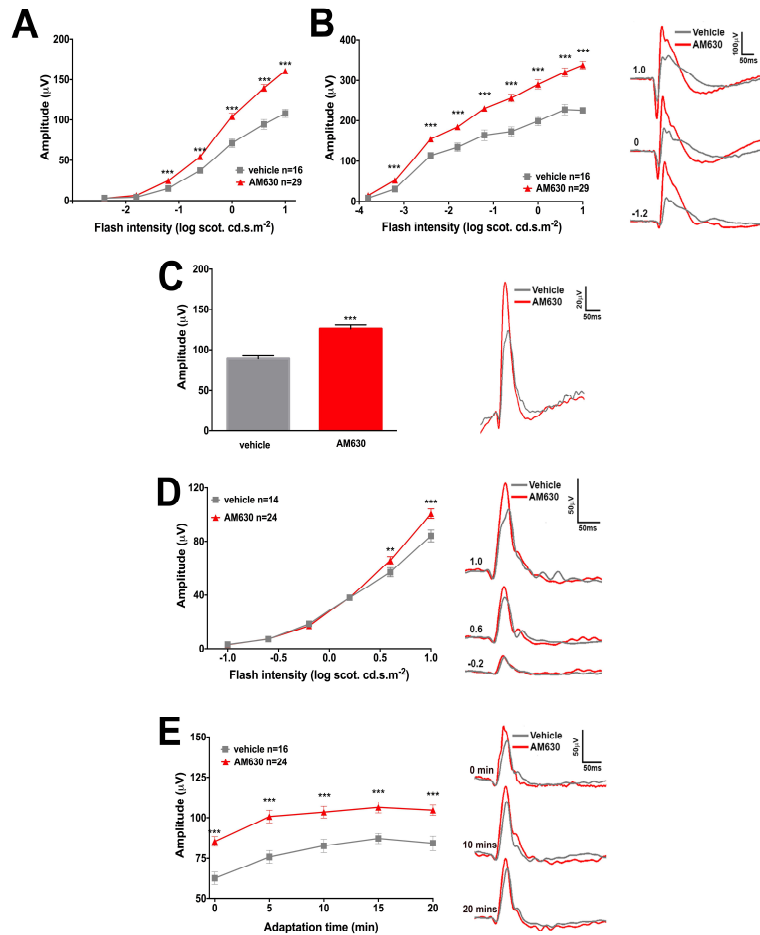


Figure 5. Prolonged treatment with CB2 antagonist recapitulates alteration of ERG seen in CB2 KO mice. Animals were treated with CB2 antagonist twice daily for seven days. A-B) Amplitudes of scotopic ERG a-wave (A) and b-wave (B) plotted as a function of flash luminance. C) Amplitudes of scotopic ERG dark adapted cone-driven response after rod saturation. D) The amplitudes of photopic ERG b-wave are plotted as a function of flash luminance. E) The amplitudes of photopic ERG b-wave are plotted as a function of time. *, $p < 0.05$, **, $p < 0.01$, ***, $p < 0.001$, 2-way ANOVA with Bonferroni post hoc test.

Chronic (1 week) pharmacological blockade of CB2 receptors in adults *does* mimic ERG alterations seen in CB2 KO mice. Genetic deletion of a receptor can have unexpected consequences, either developmental or adaptive in nature. The lack of effect of acute treatment with AM630 suggests that the altered retinal signaling seen in CB2 knockouts is due to such an adaptive or developmental effect. CB2 is intimately involved in immune function and the deletion of CB2 has been shown to enhance inflammation (Mecha et al., 2016). In order to dissect whether the altered signaling in CB2 knockouts is developmental/adaptive in nature we tested whether a prolonged weeklong blockade of CB2 receptors in adults was sufficient to mimic these changes. We found that repeated AM630 treatments twice-daily for one week recapitulated all of the consequences of CB2 genetic deletion, with enhancement of the scotopic a-wave (Fig. 5A), dark-adapted cone-driven response (Fig. 5C) and photopic b-wave (Fig. 5D,E). The treatment additionally enhanced the scotopic b-wave, which had been unaffected by CB2 deletion (Fig. 5B). We also examined whether chronic AM630 treatment altered the latencies of ERG responses. In contrast to a single treatment which had no effect on latencies, chronic treatment altered latencies in several instances. Scotopic responses were unaltered (Fig. S3A-B), but as with CB2 KOs, the photopic response was faster at the highest flash intensity (Fig S3C). This difference persisted over time (Fig. S3E). The dark-adapted cone-driven response also saw a slightly faster latency.

	CB2 KO versus WT mice at baseline
N -acyl ethanolamine	
<i>N</i> -palmitoyl ethanolamine	↓
<i>N</i> -stearoyl ethanolamine	↓
<i>N</i> -oleoyl ethanolamine	↓
<i>N</i> -linoleoyl ethanolamine	↓
<i>N</i> -arachidonoyl ethanolamine	↓
<i>N</i> -docosahexaenoyl ethanolamine	↓
N -acyl glycine	
<i>N</i> -palmitoyl glycine	↓↓
<i>N</i> -stearoyl glycine	↓↓
<i>N</i> -oleoyl glycine	↓↓
<i>N</i> -linoleoyl glycine	
<i>N</i> -arachidonoyl glycine	
<i>N</i> -docosahexaenoyl glycine	↓
N -acyl serine	
<i>N</i> -palmitoyl serine	↓↓
<i>N</i> -stearoyl serine	
<i>N</i> -oleoyl serine	↓
<i>N</i> -linoleoyl serine	
<i>N</i> -arachidonoyl serine	
<i>N</i> -docosahexaenoyl serine	
N -acyl taurine	
<i>N</i> -arachidonoyl taurine	↓
Free Fatty Acids	
Linoleic acid	↓↓↓
Arachidonic acid	↓↓
2-acyl-<i>sn</i>-glycerol	
2-arachidonoyl- <i>sn</i> -glycerol	
2-linoleoyl- <i>sn</i> -glycerol	
2-oleoyl- <i>sn</i> -glycerol	↓↓
Prostaglandins	
PGE ₂	↓↓
PGF _{2α}	↓↓
Prostaglandin E₂ 1 glyceryl ester	
PGE ₂ -G	

CB2 KO mice have lower levels of many cannabinoid-related lipids

We examined the cannabinoid-related lipid profile in eyes of CB2 KO vs. wild-type mice (n=6 biological replicates per condition). Levels of most lipids were lower (Table 2), particularly the acylethanolamines that declined as a class, though modestly. Interestingly linoleic acid and arachidonic acid both declined as did prostaglandins PGE₂ and PGF_{2α}. Levels of the endocannabinoid 2-AG were unaltered but 2-OG, a ligand at GPR119 receptors, declined.

Table 2: Levels of many cannabinoid-related lipids are lower in CB2 KO mouse eyes. LC-MS-MS measurements of cannabinoid-related lipids. Red indicates statistically significant changes. Pink indicates trend (1.0>p>0.05). Arrows indicate fold change. 1 arrow: 1-1.49; 2 arrows: 1.5-1.99; 3 arrows: 2-2.99

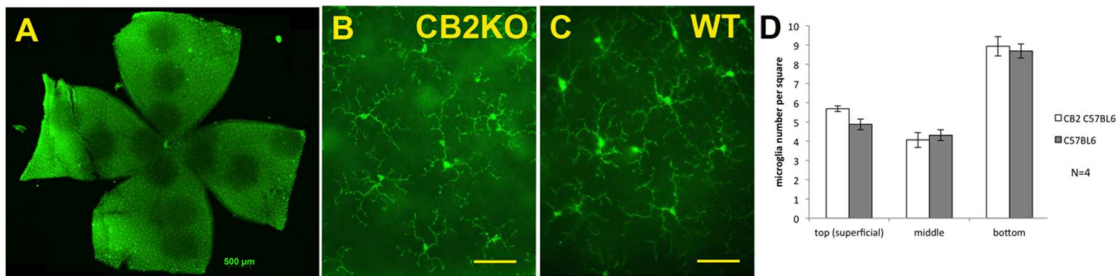


Figure 6. Microglial numbers are not altered in CB2 KO relative to wild type (WT) retina. A) Sample retina flatmount stained for Iba1. B-C) Sample image from CB2 knockout and wild type retinas showing microglial cells stained with Iba1. D) Summary shows that microglial numbers are not altered in CB2 knockouts relative to wild type retina (n=4 retinas per condition).

Microglial cell numbers and morphology are unaltered in CB2 KO mice.

CB2 receptors are chiefly found in components of the immune system including microglia and activation of CB2 generally suppresses immune cells (reviewed in (Turcotte et al., 2016)). The absence of CB2 might be expected to enhance immune responses, perhaps including microglia that are seen in retina. To explore this further we examined the numbers of retinal microglia, finding that the numbers of microglia are unaltered in CB2 knockout retina (Fig. 6D, n=4 retinae per condition). We also examined the morphology of microglia using Scholl analysis. Activated microglia are proposed to exhibit a differential, more compact morphology (reviewed in (Yu et al., 2015)). As shown in Figure 7, we did not detect a change in the number of crossings (Fig. 7, WT (n=9 cells); CB2 KO (n=11 cells); not significant by repeated measures ANOVA).

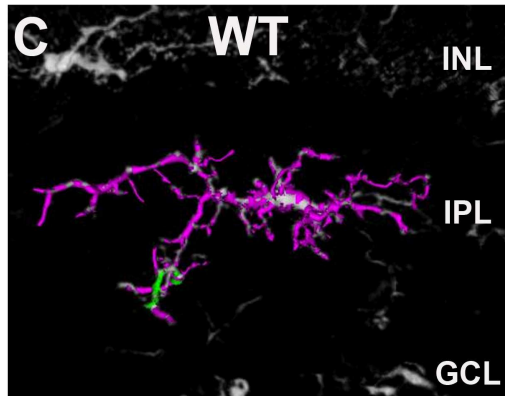
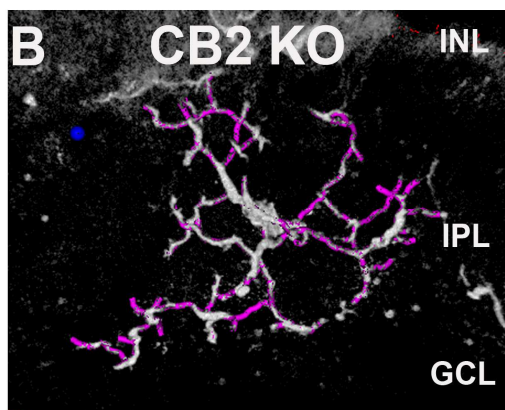
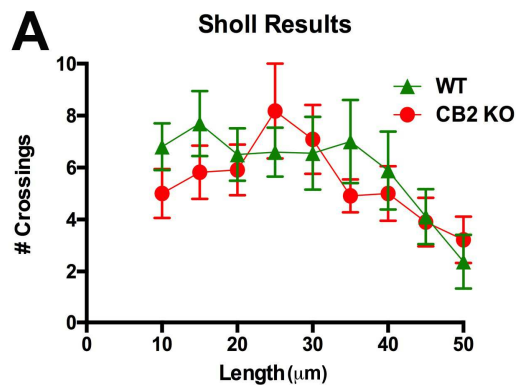


Figure 7. Microglial morphology is unaltered CB2 KO relative to wild type (WT) retina. A) Summary Sholl analysis of microglia in WT vs. CB2 knockout retina. B-C) Sample images from CB2 knockout (B, n=11) and wild type (C, n=9) retinas showing microglial cells stained with Iba1, with processes mapped and analyzed using Simple Neurite Tracer.

DISCUSSION

Our chief finding is that, consistent with published findings (Cecyre et al., 2013), cannabinoid CB2 receptor blockade impacts retinal function but that this occurs only with prolonged, not acute, block of CB2. A single treatment with CB2 antagonist AM630 is without effect while twice-daily treatment over the course of a week recapitulates the altered responses seen in CB2 knockout mice. In contrast to published findings, using a combination of immunohistochemistry and a newly developed CB2-eGFP reporter mouse, we see only minimal CB2 expression in retina under baseline conditions but CB2 appears to be upregulated in retina in response to inflammatory challenge. It remains unclear how prolonged systemic blockade of CB2 results in altered retinal signaling. The mechanism may involve altered cannabinoid metabolism since levels of many endogenous cannabinoids decline in CB2 knockouts. The changes do not appear to be due to altered number or activation of microglia as measured by Scholl analysis.

The question of what role if any the cannabinoid signaling system might play in the retina was first raised by the discovery of robust and highly conserved CB1 receptor expression in the retinae of various species ranging from salamander to primate (Straiker et al., 1999a), including humans

(Straiker et al., 1999b). This was followed by a series of in vitro studies indicating that these receptors might alter synaptic transmission at both synaptic layers (Straiker et al., 1999a; Straiker and Sullivan, 2003) as they do elsewhere in the CNS (reviewed in (Kano et al., 2009)). As discussed in the introduction the situation for CB2 was less clear partly because of contradictory studies of mRNA expression but also because the cannabinoid field has struggled to develop convincing tools to determine the expression of CB2, particularly in neurons. An ERG study showing altered light responses in CB2 knockouts but not CB1 knockouts (Cecyre et al., 2013) was therefore both surprising and intriguing.

It is broadly accepted that CB2 plays a role in immune modulation, with expression seen in several cell types of the immune system including monocytes, macrophages and microglia. CB2 activation is generally seen to suppress immune responses (reviewed in (Buckley, 2008)). Evidence for CNS expression of CB2 was largely limited to microglial expression under inflammatory conditions (e.g. (Cabral and Marciano-Cabral, 2005)) until a series of studies reporting functional CB2, chiefly in the ventral tegmental area and hippocampus (Zhang et al., 2015; Zhang et al., 2016). The above-mentioned reports of CB2-mediated alterations of neuronal function in retina were therefore a significant step in favor of a neuronal role for CB2.

The staining pattern we observed with the Cayman antibody is broadly similar to that reported by Cecyre et al. (Cecyre et al., 2014; Cecyre et al., 2013) in mouse, but is still present in CB2 knockout tissue. Cecyre et al. stated that they had tested several lots of the CB2 antibody and that staining by some antibody lots was not credible. The lot number that they published (0424681-1) was different from the lot number tested by us. So in principle, the lack of unique CB2 signal may be a function of lot-specificity. It is actually somewhat surprising that the Cayman antibody should have yielded specific staining in mouse given that it was developed against amino acids 20-33 of the human CB2 receptor. In contrast to CB1, CB2 receptors are not especially well conserved across species (~82% identity for human vs. mouse). The sequence in question differs at 4 of 14 residues (i.e. 29%) relative to the mouse CB2 receptor, making it an unlikely choice for conservation of cross-species reactivity. Indeed, the staining pattern reported using the same antibody in vervet monkey retina, for which knockouts are unavailable, was very different (Bouskila et al., 2013) even

though retinal circuitry is by and large well-maintained across species. The CB₁ staining pattern is broadly conserved in species as disparate as primate and salamander (Straiker et al., 1999a; Straiker and Sullivan, 2003). It should be noted that the CB₂ staining differs even across the two studies by Cecyre et al using the same preparation and antibody (and lot), with one showing prominent staining in the outer limiting membrane and ganglion cells (Cecyre et al., 2013), the other not (Cecyre et al., 2014). The CB₂ staining is also wholly different from that reported by Lopez et al. (2011) in rat using an antibody (aa 326-342 of rat CB₂, provided by Ken Mackie) and from that reported by Maccarone et al (2016) using an Abcam antibody. Like Cecyre et al., we have tested numerous other CB₂ antibodies in retina but have not found them to yield credible staining (e.g. Fig. S4). Our negative IHC results taken alone do not rule out retinal CB₂ expression, but it is worth noting in this context that three of four studies that examined CB₂ mRNA in retina ((Buckley et al., 1998; Porcella et al., 1998; Porcella et al., 2000) vs. (Lu et al., 2000)) did not detect CB₂. For this reason we also incorporated newly developed CB₂-eGFP reporter mice into our study. These mice produce eGFP in cells that natively express CB₂ and so serve as a useful tool to determine which cells and tissues express CB₂ though they do not offer insight into subcellular localization of those receptors since eGFP is not tethered to CB₂. Our finding that baseline expression of eGFP in these mice is minimal is consistent with the hypothesis that under baseline conditions CB₂ is expressed only modestly if at all in retina. However we did see an upregulation of eGFP after inflammatory insult with either LPS or carrageenan, thereby validating the CB₂-eGFP model for study of ocular CB₂ expression. The greatest upregulation of CB₂ however was seen in the ganglion cell layer. Changes in ganglion cell signaling would not be expected to alter the a and b waves of the ERG.

We have clarified ERG findings showing that prolonged, but not acute, block of CB₂ alters retinal signaling. But we have also offered several lines of evidence that CB₂ is minimally expressed under normal conditions in the retina. So how does this alteration of retinal signaling occur if there are few if any CB₂ receptors? Given the role of CB₂ in immune responses, alteration of some component of the ocular or systemic immune response is a possibility. To explore this we examined whether profile of endocannabinoid-related lipids was altered in the CB₂ knockout mice. We did see declines in many endocannabinoids

including the acylethanolamines that include anandamide (AEA) a likely cannabinoid receptor ligand. Since the acylethanolamines declined as a class and these lipids are produced and metabolized enzymatically this suggests that CB2 deletion alters the cannabinoid-related enzymatic profile. This could occur via upregulation of the enzyme FAAH which metabolizes this class of lipids (Cravatt et al., 2001) or perhaps downregulation of NAPE-PLD, an enzyme linked to production of these lipids (Leishman et al., 2016). Several N-arachidonoyl glycines also saw declines, but of the N-arachidonoyl glycerols, which include the endocannabinoid 2-arachidonoylglycerol (2-AG) (Sugiura et al., 1995), only 2-oleoylglycerol (2-OG) changed. 2-OG has been proposed to serve as an endogenous ligand for the GPR119 receptor (Syed et al., 2012). Because there are also changes in the levels of some free fatty acids, this may in turn impact other lipids including prostaglandins, some of which have been shown to be dependent on metabolism of endocannabinoid precursors (Nomura et al., 2011).

We separately examined whether microglia changed in numbers or morphology in CB2 knockout mice. We did see occasional CB2 positive staining in microglial-like cells in the CB2 reporter mice this was dim and very sparse. It is however consistent with evidence for CB2 expression in microglia (Stella, 2010). We quantified both the numbers of microglia and also a measure of their activation state using Scholl analysis, but saw no changes in either variable. The changed signaling may not therefore depend on altered microglial function.

Since our experiments raise questions about CB2 expression it should also be noted that cannabinoid pharmacology has also proven complicated. For instance we have shown that the nominally selective and commonly used CB2 receptor agonist JWH015 is efficacious and reasonably potent at CB1 receptors (Murataeva et al., 2012) and that the antagonist AM630 also antagonizes CB1 receptors at concentrations commonly used by researchers (Lehmann et al., 2012; Toguri et al., 2014).

In summary, while we have confirmed that CB2 deletion has consequences for retinal function, we find through a combination of functional and protein expression studies that this

is unlikely to be due to acute activation of a retinal CB2 signaling system. A prolonged (i.e. week-long) systemic blockade of CB2 receptors alters several aspects of retinal signaling but it remains to be determined how this occurs since there are few if any CB2 receptors in the retina under normal conditions. An indirect effect of systemic CB2 blockade on retinal signaling is itself an interesting finding and highlights the potential for indirect consequences of systemic drug treatments even for the relatively isolated retina.

Acknowledgements: This work was supported National Institutes of Health (grant number EY024625)

Supplementary figures

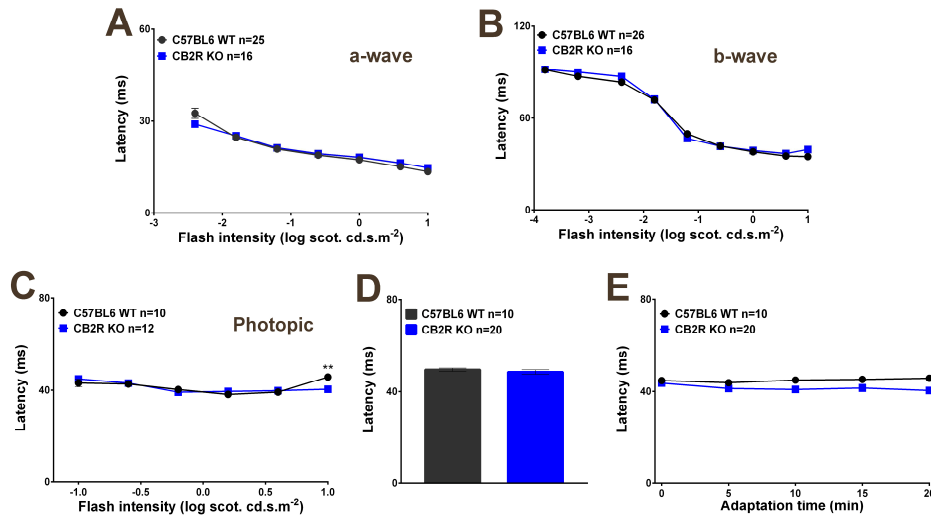


Figure S1. Latencies in CB2 KO vs. WT. A-B) Latencies for scotopic a-waves (A) and b-waves (B) in control vs. CB2 KO mice. C) Latencies for photopic responses. D) Amplitudes of scotopic ERG dark adapted cone-driven response after rod saturation. E) Latencies for b-wave plotted vs. adaptation time. *, p<0.05, **, p<0.01, ***, p<0.001, 2-way ANOVA with Bonferroni post hoc test.

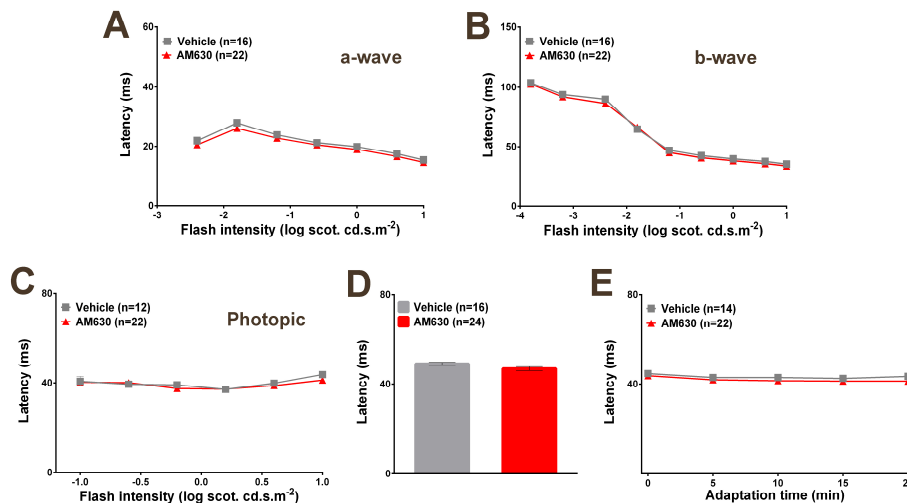


Figure S2. Latencies are unaffected by acute AM630 treatment. A-B) Latencies for scotopic a-waves (A) and b-waves (B) in control vs. AM630-treated animals. C) Latencies for photopic responses. D) Amplitudes of scotopic ERG dark adapted cone-driven response after rod saturation. E) Latencies for b-wave plotted vs. adaptation time. *, p<0.05, **, p<0.01, ***, p<0.001, 2-way ANOVA with Bonferroni post hoc test.

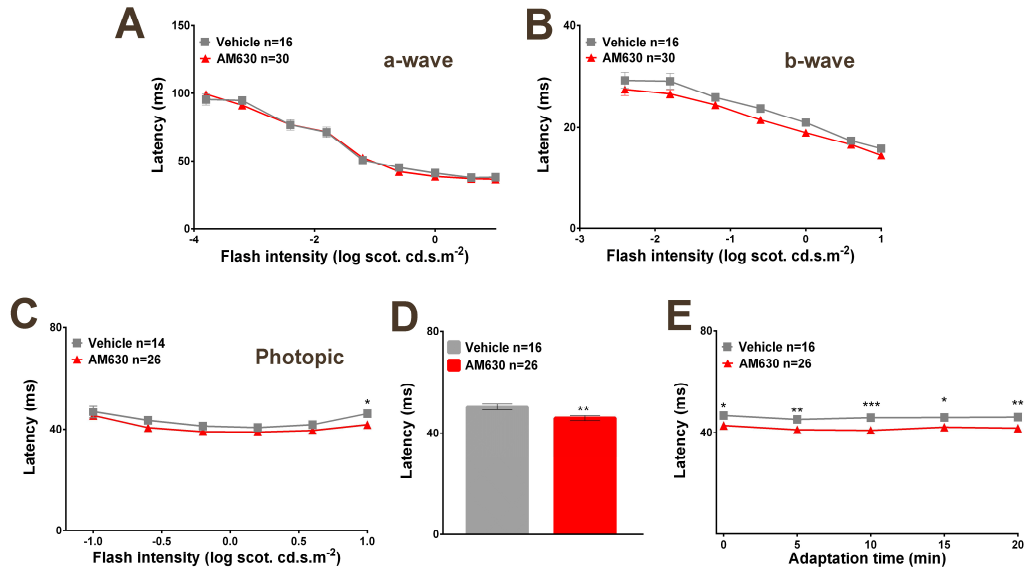


Figure S3. Latencies for chronic AM630 treatment. A-B) Latencies for scotopic a-waves (A) and b-waves (B) in control vs. AM630-treated animals. C) Latencies for photopic responses. D) Amplitudes of scotopic ERG dark adapted cone-driven response after rod saturation. E) Latencies for b-wave plotted vs. adaptation time. *, $p < 0.05$, **, $p < 0.01$, ***, $p < 0.001$, 2-way ANOVA with Bonferroni post hoc test.

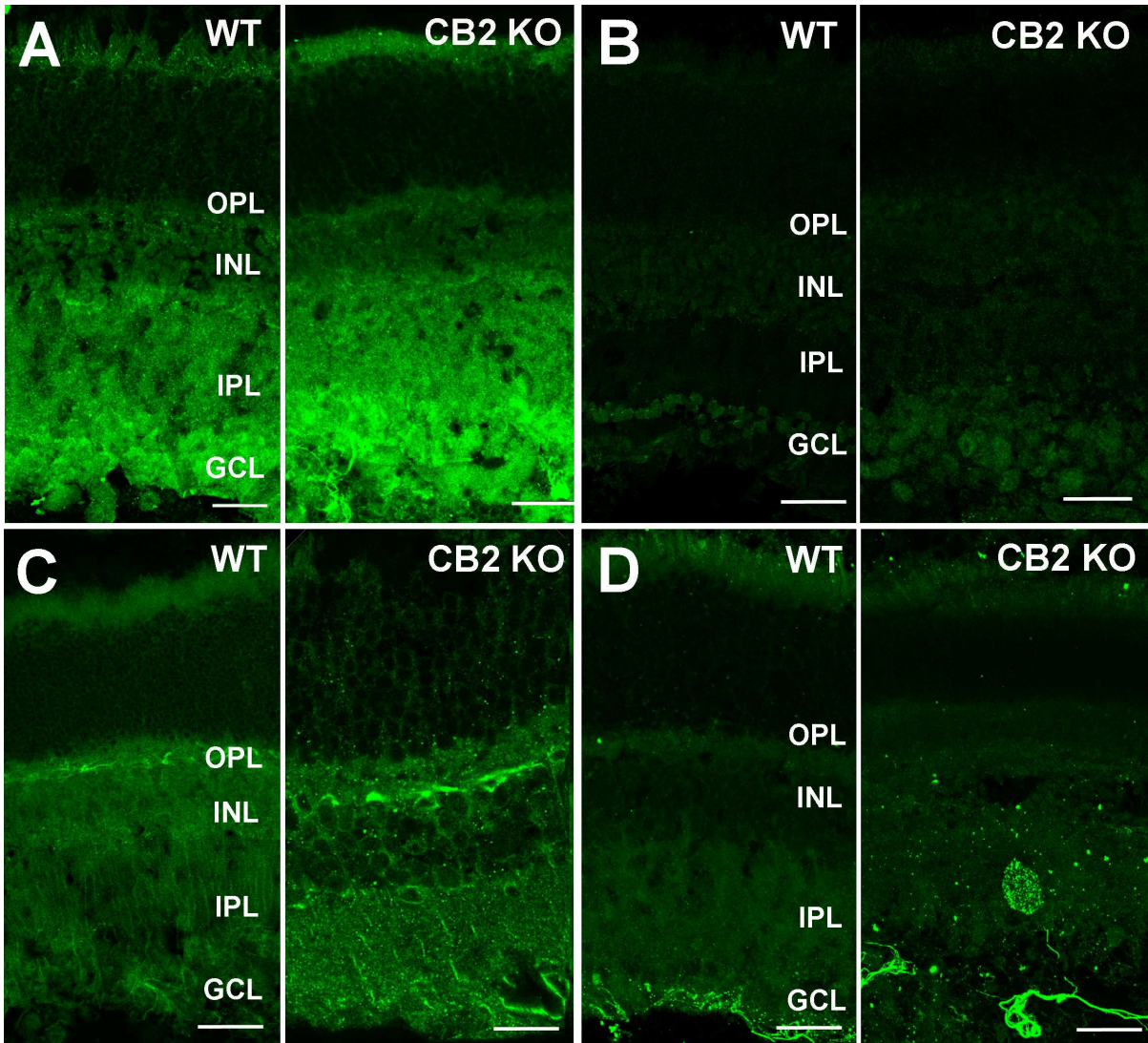


Figure S4. Testing retinal staining for CB2 antibodies with knockout controls. In addition to the Cayman antibody (Fig. 1) we tested several other commercially available CB2 antibodies including ones from A) Affinity Bioscience, B) Abcam, C) Alomone Labs, and D) Santa Cruz Biotechnology. See Table 1 for antibody details. Antibodies were tested in WT and CB2KO retina. Scale bars: 25um

LITERATURE CITED

- Atwood, B. K., Mackie, K., 2010. CB2: a cannabinoid receptor with an identity crisis. *Br J Pharmacol* 160, 467-479.
- Atwood, B. K., Straiker, A., Mackie, K., 2012. CB(2): therapeutic target-in-waiting. *Prog Neuropsychopharmacol Biol Psychiatry* 38, 16-20.
- Bouskila, J., Harrar, V., Javadi, P., Beierschmitt, A., Palmour, R., Casanova, C., Bouchard, J. F., Ptito, M., 2016. Cannabinoid Receptors CB1 and CB2 Modulate the Electroretinographic Waves in Vervet Monkeys. *Neural Plast* 2016, 1253245.
- Bouskila, J., Javadi, P., Casanova, C., Ptito, M., Bouchard, J. F., 2013. Muller cells express the cannabinoid CB2 receptor in the vervet monkey retina. *J Comp Neurol* 521, 2399-2415.
- Bradshaw, H. B., Rimmerman, N., Hu, S. S., Burstein, S., Walker, J. M., 2009. Novel endogenous N-acyl glycines identification and characterization. *Vitam Horm* 81, 191-205.
- Buckley, N. E., 2008. The peripheral cannabinoid receptor knockout mice: an update. *Br J Pharmacol* 153, 309-318.
- Buckley, N. E., Hansson, S., Harta, G., Mezey, E., 1998. Expression of the CB1 and CB2 receptor messenger RNAs during embryonic development in the rat. *Neuroscience* 82, 1131-1149.
- Cabral, G. A., Marciano-Cabral, F., 2005. Cannabinoid receptors in microglia of the central nervous system: immune functional relevance. *J Leukoc Biol* 78, 1192-1197.
- Cecyre, B., Thomas, S., Ptito, M., Casanova, C., Bouchard, J. F., 2014. Evaluation of the specificity of antibodies raised against cannabinoid receptor type 2 in the mouse retina. *Naunyn Schmiedebergs Arch Pharmacol* 387, 175-184.
- Cecyre, B., Zabouri, N., Huppe-Gourgues, F., Bouchard, J. F., Casanova, C., 2013. Roles of cannabinoid receptors type 1 and 2 on the retinal function of adult mice. *Invest Ophthalmol Vis Sci* 54, 8079-8090.
- Cravatt, B. F., Demarest, K., Patricelli, M. P., Bracey, M. H., Giang, D. K., Martin, B. R., Lichtman, A. H., 2001. Supersensitivity to anandamide and enhanced endogenous cannabinoid signaling in mice lacking fatty acid amide hydrolase. *Proc Natl Acad Sci U S A* 98, 9371-9376.
- Imamura, T., Tsuruma, K., Inoue, Y., Otsuka, T., Ohno, Y., Ogami, S., Yamane, S., Shimazawa, M., Hara, H., 2018. Involvement of cannabinoid receptor type 2 in light-induced degeneration of cells from mouse retinal cell line in vitro and mouse photoreceptors in vivo. *Exp Eye Res* 167, 44-50.
- Kano, M., Ohno-Shosaku, T., Hashimoto-dani, Y., Uchigashima, M., Watanabe, M., 2009. Endocannabinoid-mediated control of synaptic transmission. *Physiol Rev* 89, 309-380.
- Lehmann, C., Kianian, M., Zhou, J., Kuster, I., Kuschner, R., Whynot, S., Hung, O., Shukla, R., Johnston, B., Cerny, V., Pavlovic, D., Spassov, A., Kelly, M. E., 2012. Cannabinoid receptor 2 activation reduces intestinal leukocyte recruitment and systemic inflammatory mediator release in acute experimental sepsis. *Crit Care* 16, R47.
- Leishman, E., Mackie, K., Luquet, S., Bradshaw, H. B., 2016. Lipidomics profile of a NAPE-PLD KO mouse provides evidence of a broader role of this enzyme in lipid metabolism in the brain. *Biochim Biophys Acta* 1861, 491-500.

Longair, M. H., Baker, D. A., Armstrong, J. D., 2011. Simple Neurite Tracer: open source software for reconstruction, visualization and analysis of neuronal processes. *Bioinformatics* 27, 2453-2454.

Lopez, A., Aparicio, N., Pazos, M. R., Grande, M. T., Barreda-Manso, M. A., Benito-Cuesta, I., Vazquez, C., Amores, M., Ruiz-Perez, G., Garcia-Garcia, E., Beatka, M., Tolon, R. M., Dittel, B. N., Hillard, C. J., Romero, J., 2018. Cannabinoid CB2 receptors in the mouse brain: relevance for Alzheimer's disease. *J Neuroinflammation* 15, 158.

Lopez, E. M., Tagliaferro, P., Onaivi, E. S., Lopez-Costa, J. J., 2011. Distribution of CB2 cannabinoid receptor in adult rat retina. *Synapse* 65, 388-392.

Lu, Q., Straiker, A., Maguire, G., 2000. Expression of CB2 cannabinoid receptor mRNA in adult rat retina. *Vis Neurosci* 17, 91-95.

Maccarone, R., Rapino, C., Zerti, D., di Tommaso, M., Battista, N., Di Marco, S., Bisti, S., Maccarrone, M., 2016. Modulation of Type-1 and Type-2 Cannabinoid Receptors by Saffron in a Rat Model of Retinal Neurodegeneration. *PLoS ONE* 11, e0166827.

McCulloch, D. L., Marmor, M. F., Brigell, M. G., Hamilton, R., Holder, G. E., Tzekov, R., Bach, M., 2015. ISCEV Standard for full-field clinical electroretinography (2015 update). *Doc Ophthalmol* 130, 1-12.

Mecha, M., Carrillo-Salinas, F. J., Feliu, A., Mestre, L., Guaza, C., 2016. Microglia activation states and cannabinoid system: Therapeutic implications. *Pharmacol Ther*.

Murataeva, N., Mackie, K., Straiker, A., 2012. The CB2-preferring agonist JWH015 also potently and efficaciously activates CB1 in autaptic hippocampal neurons. *Pharmacol Res* 66, 437-442.

Nomura, D. K., Morrison, B. E., Blankman, J. L., Long, J. Z., Kinsey, S. G., Marcondes, M. C., Ward, A. M., Hahn, Y. K., Lichtman, A. H., Conti, B., Cravatt, B. F., 2011. Endocannabinoid hydrolysis generates brain prostaglandins that promote neuroinflammation. *Science* 334, 809-813.

Porcella, A., Casellas, P., Gessa, G. L., Pani, L., 1998. Cannabinoid receptor CB1 mRNA is highly expressed in the rat ciliary body: implications for the antiglaucoma properties of marihuana. *Brain Res Mol Brain Res* 58, 240-245.

Porcella, A., Maxia, C., Gessa, G. L., Pani, L., 2000. The human eye expresses high levels of CB1 cannabinoid receptor mRNA and protein. *Eur J Neurosci* 12, 1123-1127.

Smith, B. J., Tremblay, F., Cote, P. D., 2013. Voltage-gated sodium channels contribute to the b-wave of the rodent electroretinogram by mediating input to rod bipolar cell GABA(c) receptors. *Exp Eye Res* 116, 279-290.

Stella, N., 2010. Cannabinoid and cannabinoid-like receptors in microglia, astrocytes, and astrocytomas. *Glia* 58, 1017-1030.

Straiker, A., Stella, N., Piomelli, D., Mackie, K., Karten, H. J., Maguire, G., 1999a. Cannabinoid CB1 receptors and ligands in vertebrate retina: localization and function of an endogenous signaling system. *Proc Natl Acad Sci U S A* 96, 14565-14570.

Straiker, A., Sullivan, J. M., 2003. Cannabinoid receptor activation differentially modulates ion channels in photoreceptors of the tiger salamander. *J Neurophysiol* 89, 2647-2654.

Straiker, A. J., Maguire, G., Mackie, K., Lindsey, J., 1999b. Localization of cannabinoid CB1 receptors in the human anterior eye and retina. *Invest Ophthalmol Vis Sci* 40, 2442-2448.

Sugiura, T., Kondo, S., Sukagawa, A., Nakane, S., Shinoda, A., Itoh, K., Yamashita, A., Waku, K., 1995. 2-Arachidonoylglycerol: a possible endogenous cannabinoid receptor ligand in brain. *Biochem Biophys Res Commun* 215, 89-97.

Syed, S. K., Bui, H. H., Beavers, L. S., Farb, T. B., Ficorilli, J., Chesterfield, A. K., Kuo, M. S., Bokvist, K., Barrett, D. G., Efanov, A. M., 2012. Regulation of GPR119 receptor activity with endocannabinoid-like lipids. *Am J Physiol Endocrinol Metab* 303, E1469-1478.

Toguri, J. T., Caldwell, M., Kelly, M. E., 2016. Turning Down the Thermostat: Modulating the Endocannabinoid System in Ocular Inflammation and Pain. *Front Pharmacol* 7, 304.

Toguri, J. T., Lehmann, C., Laprairie, R. B., Szczesniak, A. M., Zhou, J., Denovan-Wright, E. M., Kelly, M. E., 2014. Anti-inflammatory effects of cannabinoid CB(2) receptor activation in endotoxin-induced uveitis. *Br J Pharmacol* 171, 1448-1461.

Toguri, J. T., Moxsom, R., Szczesniak, A. M., Zhou, J., Kelly, M. E., Lehmann, C., 2015. Cannabinoid 2 receptor activation reduces leukocyte adhesion and improves capillary perfusion in the iridial microvasculature during systemic inflammation. *Clin Hemorheol Microcirc* 61, 237-249.

Turcotte, C., Blanchet, M. R., Laviolette, M., Flamand, N., 2016. The CB2 receptor and its role as a regulator of inflammation. *Cell Mol Life Sci* 73, 4449-4470.

Yu, Y., Chen, H., Su, S. B., 2015. Neuroinflammatory responses in diabetic retinopathy. *J Neuroinflammation* 12, 141.

Zhang, H. Y., Bi, G. H., Li, X., Li, J., Qu, H., Zhang, S. J., Li, C. Y., Onaivi, E. S., Gardner, E. L., Xi, Z. X., Liu, Q. R., 2015. Species differences in cannabinoid receptor 2 and receptor responses to cocaine self-administration in mice and rats. *Neuropsychopharmacology* 40, 1037-1051.

Zhang, H. Y., Gao, M., Shen, H., Bi, G. H., Yang, H. J., Liu, Q. R., Wu, J., Gardner, E. L., Bonci, A., Xi, Z. X., 2016. Expression of functional cannabinoid CB2 receptor in VTA dopamine neurons in rats. *Addict Biol*.

	CB2 KO versus WT mice at baseline
N-acyl ethanolamine	
<i>N</i> -palmitoyl ethanolamine	↓
<i>N</i> -stearoyl ethanolamine	↓
<i>N</i> -oleoyl ethanolamine	↓
<i>N</i> -linoleoyl ethanolamine	↓
<i>N</i> -arachidonoyl ethanolamine	↓
<i>N</i> -docosahexaenoyl ethanolamine	↓
N-acyl glycine	
<i>N</i> -palmitoyl glycine	↓↓
<i>N</i> -stearoyl glycine	↓↓
<i>N</i> -oleoyl glycine	↓↓
<i>N</i> -linoleoyl glycine	
<i>N</i> -arachidonoyl glycine	
<i>N</i> -docosahexaenoyl glycine	↓
N-acyl serine	
<i>N</i> -palmitoyl serine	↓↓
<i>N</i> -stearoyl serine	
<i>N</i> -oleoyl serine	↓
<i>N</i> -linoleoyl serine	
<i>N</i> -arachidonoyl serine	
<i>N</i> -docosahexaenoyl serine	
N-acyl taurine	
<i>N</i> -arachidonoyl taurine	↓
Free Fatty Acids	
Linoleic acid	↓↓↓
Arachidonic acid	↓
2-acyl-sn-glycerol	
2-arachidonoyl-sn-glycerol	
2-linolenoyl-sn-glycerol	
2-oleoyl-sn-glycerol	↓↓
Prostaglandins	
PGE ₂	↓↓
PGF _{2a}	↓↓
Prostaglandin E2 1 glyceryl ester	
PGE ₂ -G	